



OPEN ACCESS

EDITED BY

Dongchan Jang,
Korea Advanced Institute of Science and
Technology (KAIST), South Korea

REVIEWED BY

Emanuele Reccia,
University of Cagliari, Italy
Jianyong Han,
Shandong Jianzhu University, China
Yue Zhao,
Shandong University of Science and
Technology, China

*CORRESPONDENCE

Gaojian Hu,
hugaojian8@163.com

SPECIALTY SECTION

This article was submitted to Mechanics
of Materials,
a section of the journal
Frontiers in Materials

RECEIVED 12 July 2022

ACCEPTED 03 October 2022

PUBLISHED 24 October 2022

CITATION

Zhang J, Guo W, Fu Y, Feng Y, Wang Q,
Hu G and Wang T (2022), Study on the
size effect of the secant modulus of
rocks containing multiple parallel joints.
Front. Mater. 9:992133.
doi: 10.3389/fmats.2022.992133

COPYRIGHT

© 2022 Zhang, Guo, Fu, Feng, Wang, Hu
and Wang. This is an open-access article
distributed under the terms of the
[Creative Commons Attribution License
\(CC BY\)](https://creativecommons.org/licenses/by/4.0/). The use, distribution or
reproduction in other forums is
permitted, provided the original
author(s) and the copyright owner(s) are
credited and that the original
publication in this journal is cited, in
accordance with accepted academic
practice. No use, distribution or
reproduction is permitted which does
not comply with these terms.

Study on the size effect of the secant modulus of rocks containing multiple parallel joints

Jing Zhang¹, Wannian Guo¹, Yongzhi Fu², Yong Feng²,
Qingxia Wang¹, Gaojian Hu^{3,4*} and Tao Wang¹

¹College of Safety and Emergency Management Engineering, Taiyuan University of Technology, Taiyuan, Shanxi, China, ²Yanbao Energy, China Energy Investment, Hulun Buir, China, ³School of Civil Engineering, Shaoxing University, Shaoxing, Zhejiang, China, ⁴Key Laboratory of Rock Mechanics and Geohazards of Zhejiang Province, Shaoxing, Zhejiang, China

The secant modulus of the rock reflects the stiffness of the rock and the ability to resist deformation. There are significant differences in the secant modulus of the rock due to the different numbers of joints in the rock and the change in rock size. Therefore, it is important to obtain effectively the secant modulus of rocks with the number of parallel joints for evaluating rock deformation. In this study, the method of regression analysis is used, and 10 sets of numerical plans are set up to discuss the influence of a number of parallel joints and rock size on the secant modulus. The results show that the secant modulus decreases with the increase in a number of parallel joints, and the curve is a power function. The secant modulus decreases when the rock size increases, and the curve is an exponential function. The characteristic secant modulus and characteristic size decrease with the increase in the number of parallel joints, and their curves are an exponential function. The specific forms of these relationships are given in the article. The establishment of these relationships realizes the prediction and calculation of the rock secant modulus with the number of parallel joints, which provides a guiding significance for the rock deformation analysis.

KEYWORDS

size effect, characteristic size, parallel joint, secant modulus, characteristic secant modulus

1 Introduction

The secant modulus is the slope of the line connecting the point corresponding to the 50% compressive strength and the origin on the stress-strain curve of the rock under unidirectional stress (Briaud, 2001). It can reflect the stiffness of the rock, and its increase can reflect the increase in the material's ability to resist deformation to a certain extent (Ahn et al., 2015). Therefore, the secant modulus is a very important parameter index, which is of great significance in analyzing the laws of rock deformation and failure, and plays an important role in guiding the design, construction, and stability of underground engineering (Wang et al., 2021).

The joints in the rock affect the secant modulus. For example, there are parallel joints in some sedimentary rocks, which significantly affect the secant modulus. At the same

TABLE 1 Simulation plans (Mahdevari et al., 2020).

Simulation plan	NPJ	Plan 1	Plan 2	Plan 3	Plan 4	Plan 5
		$l = 100 \text{ mm}$	$l = 200 \text{ mm}$	$l = 400 \text{ mm}$	$l = 600 \text{ mm}$	$l = 800 \text{ mm}$
Plan 6	2	2×100	2×200	2×400	2×600	2×800
Plan 7	4	4×100	4×200	4×400	4×600	4×800
Plan 8	6	6×100	6×200	6×400	6×600	6×800
Plan 9	8	8×100	8×200	8×400	8×600	8×800

where l is the rock size.

TABLE 2 Mechanical parameters of the rock (Mahdevari et al., 2020).

Material	Elastic modulus [MPa]	Uniaxial compressive strength [MPa]	Poisson's ratio	Friction angle [°]
Rock	4874	101.34	0.25	48.32
Joint	1.1	1.5	0.30	30

time, the number of parallel joints (NPJs) existing in the rock will cause the difference in the secant modulus (Li et al., 2020), for example, Zhang (2009) studied the influence of the joint number on the secant modulus based on the micro-deformation characteristics of the fractured rock mass. Scholars have studied the effects of rock temperature, confining pressure, and saturation on the secant modulus. In terms of temperature, Zhao et al. (2017) determined the empirical coefficient of the secant modulus by the inverse analysis method. Zhang et al. (2021) established the constitutive relation of the broken coal body considering the temperature by fitting the relationship between the secant modulus of the broken coal body and the temperature under the action of stress. Su et al. (2017) studied the effect of temperature and pulse angle on the secant modulus through a triaxial compression test. Erisa et al. (2021) studied the effect of loading frequency on the secant modulus of concrete and explored the source of temperature increase. In the effect of confining pressure on the secant modulus, for example, Kang et al. (2018) defined the damage coefficient according to the secant modulus attenuation characteristics and compared the influence of confining pressure on the secant modulus and damage evolution characteristics. Zhang et al. (2020) carried out numerical construction of porous coal samples and analyzed the secant modulus of porous samples considering pore density and confining pressure. Hang-Zhou and Liao (2007) analyzed the relationship between the secant modulus and internal friction angle of expansive mudstone, confining pressure. Uniaxial compression laboratory tests and numerical tests are commonly used test methods to study the secant modulus, for example, studied the uniaxial compressive strength and the

secant modulus of the hardened cement slurry with different water saturation levels through a uniaxial compression test. Zhang and Zhu (2020) conducted uniaxial compression simulation experiments on prefabricated rock-like materials by Particle Flow Code (PFC) software and obtained the laws of mechanical parameters such as the secant modulus of different samples. Nouri et al. (2016) explored the effect of plastic enhancement behavior on the secant modulus in sandstone through a triaxial compression test. Asgari et al. (2015) studied the relationships between the secant modulus and UCS, curing time, and cement. The aforementioned studies have obtained the relation between the secant modulus and temperature, confining pressure, and saturation. However, there are NPJs in the rock, and the existence of parallel joints has an important influence on the strength of the rock (Hu et al., 2022a). Therefore, it is important to explore the effect of parallel joints in rocks on the secant modulus and to obtain the relationship between the two. In this regard, scholars have carried out relatively little research.

The rock has a size effect, and the change in rock size will also affect the secant modulus. For example, the change in the size of some sedimentary rocks rich in joints will affect the change in the rock secant modulus, for example, Ban et al. (2019) characterized the mechanical properties with the size effect based on the secant modulus method and the effective mode reduction method. In addition, scholars have also carried out research on the size effect of the secant modulus from the perspectives of rock aspect ratio, particle size, and joint length, for example, Sun et al. (2022) studied the aspect ratio effect of the dynamic deformation modulus of coal and found that the sensitivity of the secant modulus strain rate in the plastic section of the specimen with a

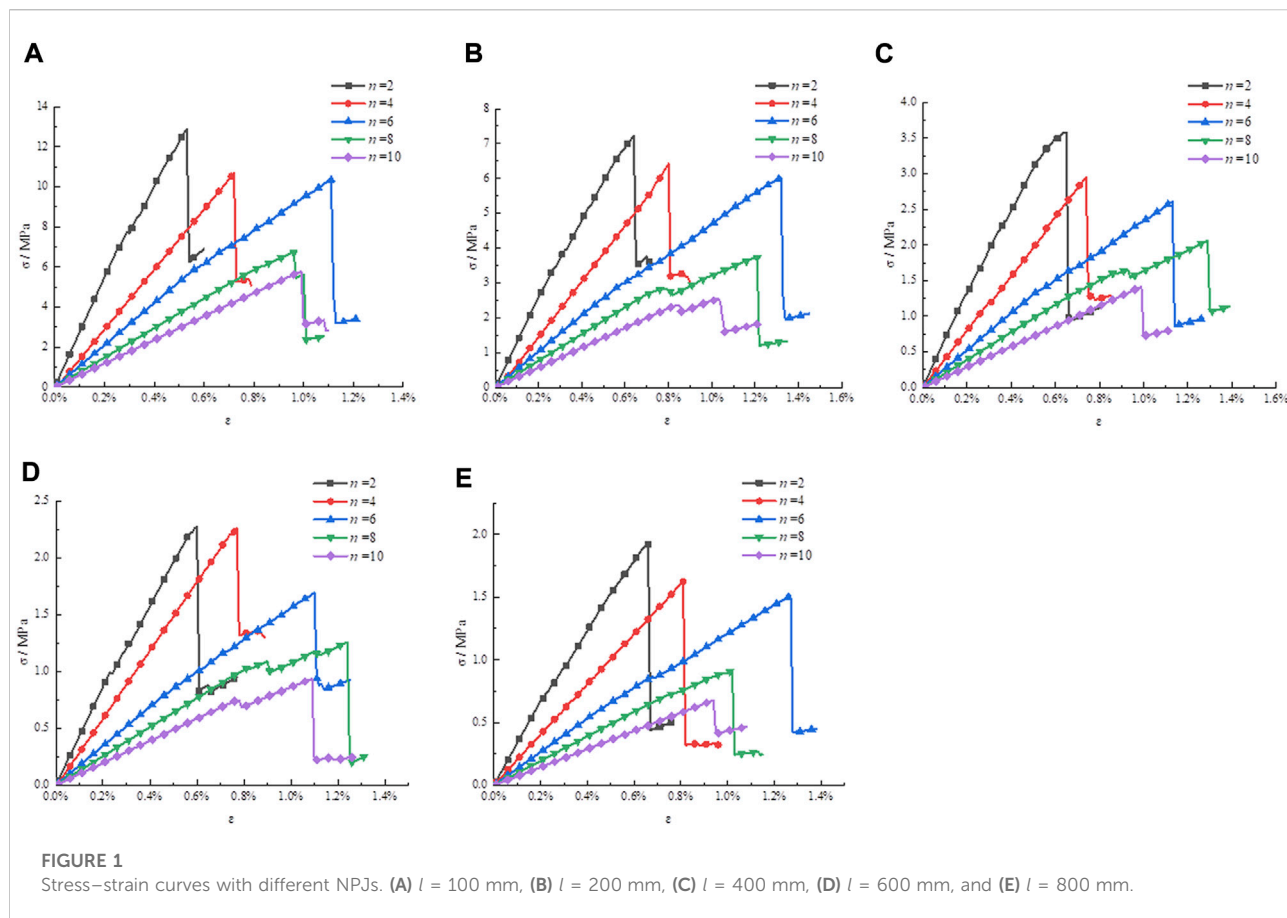


TABLE 3 Secant modulus.

Numerical simulation	Rock size [mm]	Secant modulus [GPa]				
		Plan 6	Plan 7	Plan 8	Plan 9	Plan 10
		$n = 2$	$n = 4$	$n = 6$	$n = 8$	$n = 10$
Plan 1	100	2.746	1.467	1.053	0.739	0.591
Plan 2	200	1.233	0.763	0.499	0.383	0.285
Plan 3	400	0.642	0.388	0.261	0.194	0.143
Plan 4	600	0.409	0.296	0.170	0.128	0.097
Plan 5	800	0.308	0.202	0.130	0.098	0.072

Here, n is the number of parallel joints.

large aspect ratio is stronger than that of the specimen with a small aspect ratio. Mahdevari et al. (2020) studied the effect of bulk size and bulk volume ratio on the deformation modulus by making large-scale physical samples. Davarpanah et al. (2020) studied the effect of the modulus ratio on the rock modulus and explored the validity of the mathematical model proposed by Zhu

(2021) by PFC software to obtain the stress–strain curves of the substitute materials at all levels and found that there was an exponential correlation between the ratio of the secant modulus and the maximum particle size D of the sample. Liu et al. (2020) conducted uniaxial compression tests on rock samples with rough joints to study the effect of joint length on the secant

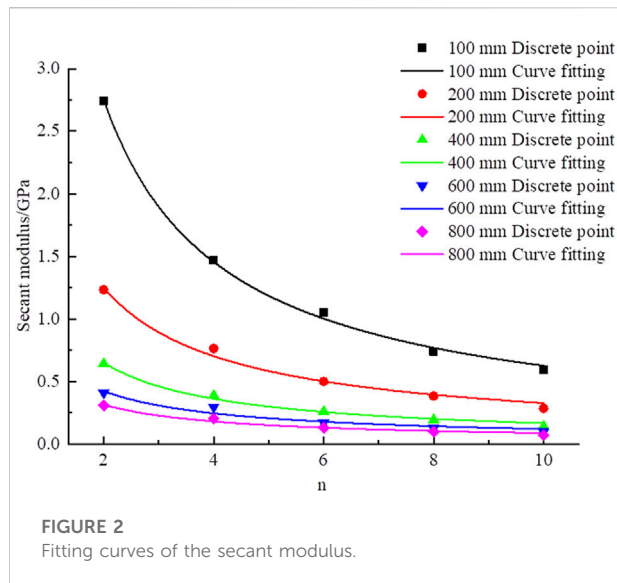


FIGURE 2
Fitting curves of the secant modulus.

TABLE 4 Fitting relationship between the secant modulus and NPJs.

Rock size [mm]	Fitting formula	Fitting coefficient [R^2]
100	$E_{50}(n) = 5.21n^{-0.92}$	0.998
200	$E_{50}(n) = 2.23n^{-0.883}$	0.990
400	$E_{50}(n) = 1.172n^{-0.848}$	0.991
600	$E_{50}(n) = 0.731n^{-0.788}$	0.948
800	$E_{50}(n) = 0.55n^{-0.755}$	0.980

Here, $E_{50}(n)$ [GPa] is E_{50} when the NPJs is n .

modulus, cracking process, and failure mode. Majdi and Beiki (2019) proposed a prediction method to determine the deformation modulus of the rock by means of multiple regression analysis. The aforementioned research has gotten the size effect of the secant modulus from different angles, indicating that there is indeed a size effect on the rock secant modulus. Therefore, when there are parallel joints in the rock, the size effect of the secant modulus still exists. NPJs often occur in rocks, so it is particularly important in engineering to explore the size effect of the secant modulus of rocks with NPJs and to obtain the relation between the secant modulus and size. However, there is still relatively little research in this area.

Different rock sizes have an impact on the surface area of rock weathering. Therefore, it is particularly important to determine the rock's characteristic size. The study of the rock size effect is important to prevent erosion in rivers, oceans, and glaciers and analyze bulk rock size in hilly terrain. Some scholars have carried out some research on the study of REV. For example, Loyola et al. (2021) presented a new general methodology to define the size of the REV for the geometrical

and elastic moduli of fractured media. Peng et al. (2020) analyzed the size effect through PFC software and obtained a REV size of 16 m. Hu et al. (2022b) obtained the relation between the spacing of parallel joints and elastic modulus characteristic size. In the study of the secant modulus of REV, Zhang (2013) obtained the REV of the deformation parameters and strength parameters of the rock mass through numerical tests of rock mass samples of different sizes. The aforementioned studies show that there are relatively few studies on the secant modulus in terms of the REV of rock mechanical parameters, especially the secant modulus of rocks with parallel joints.

In the study, the effect of rock size and NPJs on E_{50} is explored. The relationships between E_{50} and NPJs, E_{50} and rock size, the characteristic size of rock E_{50} and NPJs, and the rock characteristic E_{50} and NPJs are established.

2 Numerical simulation plans

The research content is divided into two aspects: 1) influence of the NPJs on E_{50} ; NPJs are 2, 4, 6, 8, and 10, including plans 1–5; and 2) influence of rock size with NPJs on E_{50} , whose rock sizes are 100 mm, 200 mm, 400 mm, 600 mm, and 800 mm, including plans 6–10. A two-dimensional numerical model was used in the study with a height-to-diameter ratio of 1:1. Simulation plans (Mahdevari et al., 2020) are shown in Table 1.

In the research, RFPA software was used to carry out uniaxial compression simulation research based on the uniaxial compression deformation theory of rocks. RFPA is a rock fracture process analysis system with elastic mechanics as the stress analysis tool and elastic damage theory and its modified Coulomb failure criterion as the medium deformation and failure analysis module. The basic principle of the program can be summarized as follows: first, the rock medium model is discretized into a numerical model composed of mesoscopic primitives. Then, it is assumed that the mechanical properties of the discretized mesoscopic primitives obey the Weibull distribution, and the connection between the mesoscopic and macroscopic media is established. Based on the linear elastic finite element analysis method, the basic element failure criterion and damage law are introduced to solve the problem, and the deformation and failure process of the rock is obtained.

Displacement loading was applied along the upper surface of the model with a loading increment of 0.01 mm, and no load was applied on both sides of the model (Mahdevari et al., 2020). The rock mechanics parameters used in the simulation are shown in Table 2. A regression analysis method was used in the study. The basic idea of regression analysis is to solve a series of secant modulus values based on numerical models, mathematically process the data values to obtain a series of parameters, and establish the corresponding regression equations.

TABLE 5 Value of parameters a and b.

Parameter	$l = 100 \text{ mm}$	$l = 200 \text{ mm}$	$l = 400 \text{ mm}$	$l = 600 \text{ mm}$	$l = 800 \text{ mm}$
a	5.210	2.230	1.172	0.731	0.550
b	-0.920	-0.883	-0.848	-0.788	-0.755

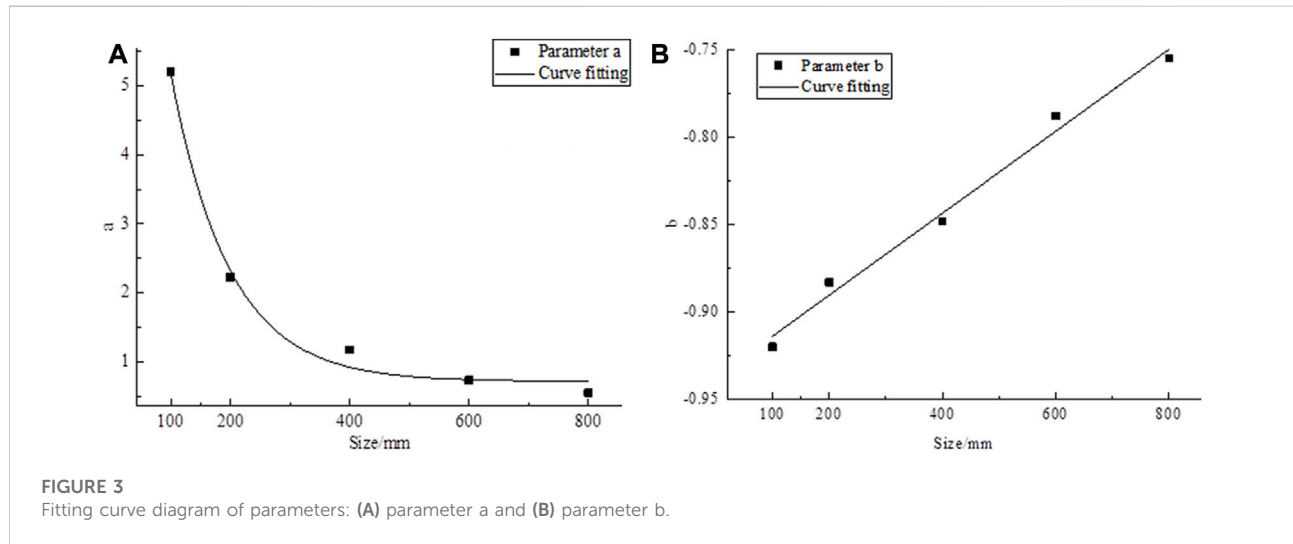


FIGURE 3 Fitting curve diagram of parameters: (A) parameter a and (B) parameter b.

3 Numerical simulation results

3.1 Influence of the NPJs on E_{50}

3.1.1 Rock stress law of different NPJs

From the research content (1), the stress–strain curves in plans 1–5 are drawn in Figure 1.

Figures 1A–E indicate that the obtained patterns of the curves do not considerably vary with the variation of rock size. Therefore, one of the pictures is chosen to describe the failure law when NPJs change.

The rock size in Figure 1B is 200 mm. In Figure 1B, when the NPJs are 2, 4, 6, 8, and 10, the obtained stress–strain curves are very similar. These curves gradually change from linear elastic deformation to plastic failure, and the curves conform to the general law of rock failure. Figure 1B shows that when the rock size is 200 mm, as the NPJs change from 2 to 10, the peak strength decreases. The main reason is that when the NPJs increase, the damage value of the rock increases under the same strain value, and the rock resistance to deformation and destruction decreases continuously. The peak strength is connected with the NPJs.

3.1.2 Fitting method for the secant modulus and NPJs

According to the stress–strain curves in Figure 1, the point of 50% compressive strength was selected, the slope of the line connecting it with the origin was calculated, and E_{50} of the rock under each working condition was obtained, as shown in Table 3.

A scatter plot of E_{50} and NPJs in Table 3 is drawn, and their fitting curves are regressed, as shown in Figure 2.

Figure 2 indicates that when the NPJs is six, E_{50} of the rock decreases from 1.053 GPa to 0.13 GPa with the increase in the rock size from 100 mm to 800 mm, which indicates that E_{50} of the rock is affected by the rock size and decreases with the increase in the rock size. This law is similar even if the NPJs are different. When the rock size is 100 mm, the NPJs increase from 2 to 10, and E_{50} of the rock decreases from 2.746 GPa to 0.591 GPa, which indicates that rock E_{50} decreases with the increase in the NPJs.

The aforementioned observations show that E_{50} is in connection with the NPJs and rock size. In order to better illustrate this relationship, the formula of the regression curves is listed in Table 4.

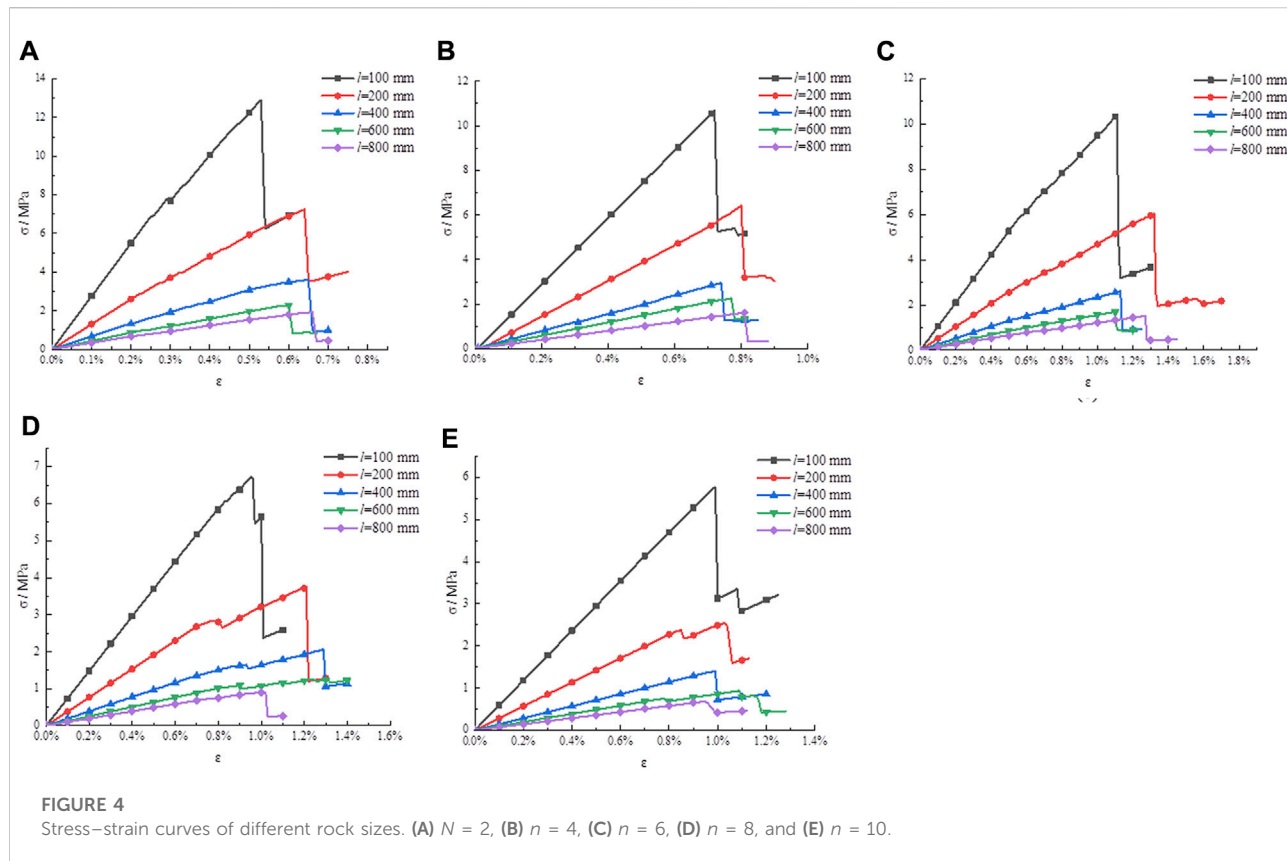


TABLE 6 Secant modulus.

Numerical simulation	Number of parallel joints	Secant modulus [GPa]				
		Plan 1	Plan 2	Plan 3	Plan 4	Plan 5
		$l = 100 \text{ mm}$	$l = 200 \text{ mm}$	$l = 400 \text{ mm}$	$l = 600 \text{ mm}$	$l = 800 \text{ mm}$
Plan 6	2	2.746	1.233	0.642	0.409	0.308
Plan 7	4	1.467	0.763	0.388	0.296	0.202
Plan 8	6	1.053	0.499	0.261	0.170	0.130
Plan 9	8	0.739	0.383	0.194	0.128	0.098
Plan 10	10	0.591	0.285	0.143	0.097	0.072

3.1.3 Relationship between the secant modulus and NPJs

From the data fitting results in Table 4, the curve trend of E_{50} and NPJs is a power function, and the resulting mathematical model is as follows:

$$E_{50}(n) = an^b, \tag{1}$$

where $E_{50}(n)$ [GPa] is E_{50} when the NPJs is n , n is NPJs, and a and b are parameters.

From the expressions obtained in Table 4, the parameters a and b can be extracted, and the values of each parameter are shown in Table 5. Each parameter is fitted with the rock size, and the fitting curve obtained is shown in Figure 3.

From the curve obtained in Figure 3, each parameter has a certain relationship with the size, and the expression is as follows:

$$a = 0.714 + 12.437e^{-0.01l}, \tag{2}$$

$$b = 2.344n - 0.937. \tag{3}$$

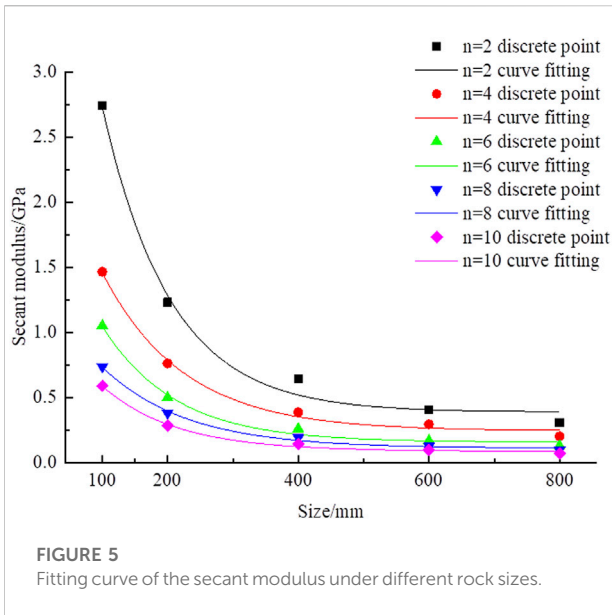


FIGURE 5 Fitting curve of the secant modulus under different rock sizes.

From Eqs 1–3, the expression between E_{50} and NPJs can be obtained as

$$E_{50}(n) = (0.714 + 12.437e^{-0.011})n^{2.344n-0.937}. \quad (4)$$

Eq. 4 is a special relational formula used to solve the corresponding rock E_{50} when the NPJs change, and its applicable condition is a two-dimensional plane strain. For the engineering site, when the size of the rock used for research is determined, the corresponding rock E_{50} value can be quickly obtained according to the NPJs existing in the rock. This relationship quantifies and simplifies the solution of E_{50} of rocks with parallel joints.

3.2 Influence of the rock size on the rock secant modulus

3.2.1 Rock stress law of different rock sizes

From the research content (2), the stress–strain curves in plans 6–10 are drawn in Figure 4.

Figures 4A–E show that the obtained patterns of the curves do not considerably vary with the change of the NPJs. Therefore, one of the pictures is chosen to describe the failure law when the rock size changes.

The NPJs in Figure 4E is 10. In Figure 4E, when the rock size is increased from 100 mm to 800 mm, the obtained stress–strain curves have very similar regularity. These curves gradually change from linear elastic deformation to plastic failure, and the curves conform to the general law of rock failure. Figure 4E shows that the NPJs is 10; as the rock size increases from 100 mm to 800 mm, the peak strength of the rock decreases. It shows that the rock’s peak strength is connected with the rock size.

3.2.2 Fitting method for the secant modulus and rock size

From the stress–strain curves in Figure 4, the point of 50% compressive strength was selected, the slope of the line connecting it with the origin was calculated, and E_{50} of the rock was obtained, as shown in Table 6.

A scatter diagram of E_{50} and rock size in Table 6 is plotted, and their fitting curves are regressed, as shown in Figure 5.

Figure 5 indicates that as the rock size is 100 mm, the NPJs increase from 2 to 10, and rock E_{50} decreases from 2.746 GPa to 0.591 GPa, which indicates that rock E_{50} decreases with the increase in the NPJs. This law is the same even if rock sizes become different. When the NPJs is four, E_{50} of rocks decreases from 1.467 GPa to 0.202 GPa with the increase in the rock size from 100 mm to 800 mm, which indicates that E_{50} of rocks is connected with the rock size and decreases with the increase in the rock size.

To better analyze the relation between E_{50} and the rock size, the functional formula of the fitting curves in Figure 5 is listed in Table 7.

3.2.3 Relationship between the secant modulus and rock size

From the data fitting results in Table 7, the curve trend of E_{50} and rock size is an exponential function, and the resulting mathematical model is as follows:

$$E_{50}(l) = d + fe^{-gl}, \quad (5)$$

TABLE 7 Fitting relationship of the secant modulus.

Number of parallel joints	Fitting formula	Fitting coefficient [R^2]
2	$E_{50}(l) = 0.389 + 6.132e^{-0.0096l}$	0.993
4	$E_{50}(l) = 0.245 + 2.722e^{-0.0091l}$	0.995
6	$E_{50}(l) = 0.158 + 2.184e^{-0.009l}$	0.994
8	$E_{50}(l) = 0.111 + 1.362e^{-0.0089l}$	0.996
10	$E_{50}(l) = 0.088 + 1.209e^{-0.0088l}$	0.997

TABLE 8 Values of parameters d , f , and g .

Parameter	$n = 2$	$n = 4$	$n = 6$	$n = 8$	$n = 10$
d	0.389	0.245	0.158	0.111	0.088
f	6.132	2.722	2.184	1.362	1.209
g	0.0096	0.0091	0.0090	0.0089	0.0088

where $E_{50}(l)$ [GPa] is the E_{50} value of the rock when the rock size is l , l [mm] is the rock size, and d , f , and g are parameters.

From the expressions obtained in Table 7, the values of parameters d , f , and g can be extracted, and the values of each parameter are shown in Table 8. Each parameter is fitted with the NPJs, and the fitting curve obtained is shown in Figure 6.

From the curve obtained in Figure 6, each parameter has a certain relationship with the NPJs, and the expression is as follows:

$$d = 0.714l^{-0.848}, \tag{6}$$

$$f = 12.522l^{-1.04}, \tag{7}$$

$$g = 0.00185e^{-0.434l} + 0.0088. \tag{8}$$

From Eqs 5–8, the expression between E_{50} and rock size can be obtained as

$$E_{50}(l) = 12.522l^{-1.04}e^{-0.00185e^{-0.434l}-0.0088l} + 0.714l^{-0.848}. \tag{9}$$

Eq. 9 is a special relational formula used to solve the corresponding rock E_{50} value when the rock size changes, and its applicable condition is a two-dimensional plane strain. When the NPJs in a rock are known, its E_{50} changes with the variation in the rock size. Eq. 9 gives the characteristics of this change and

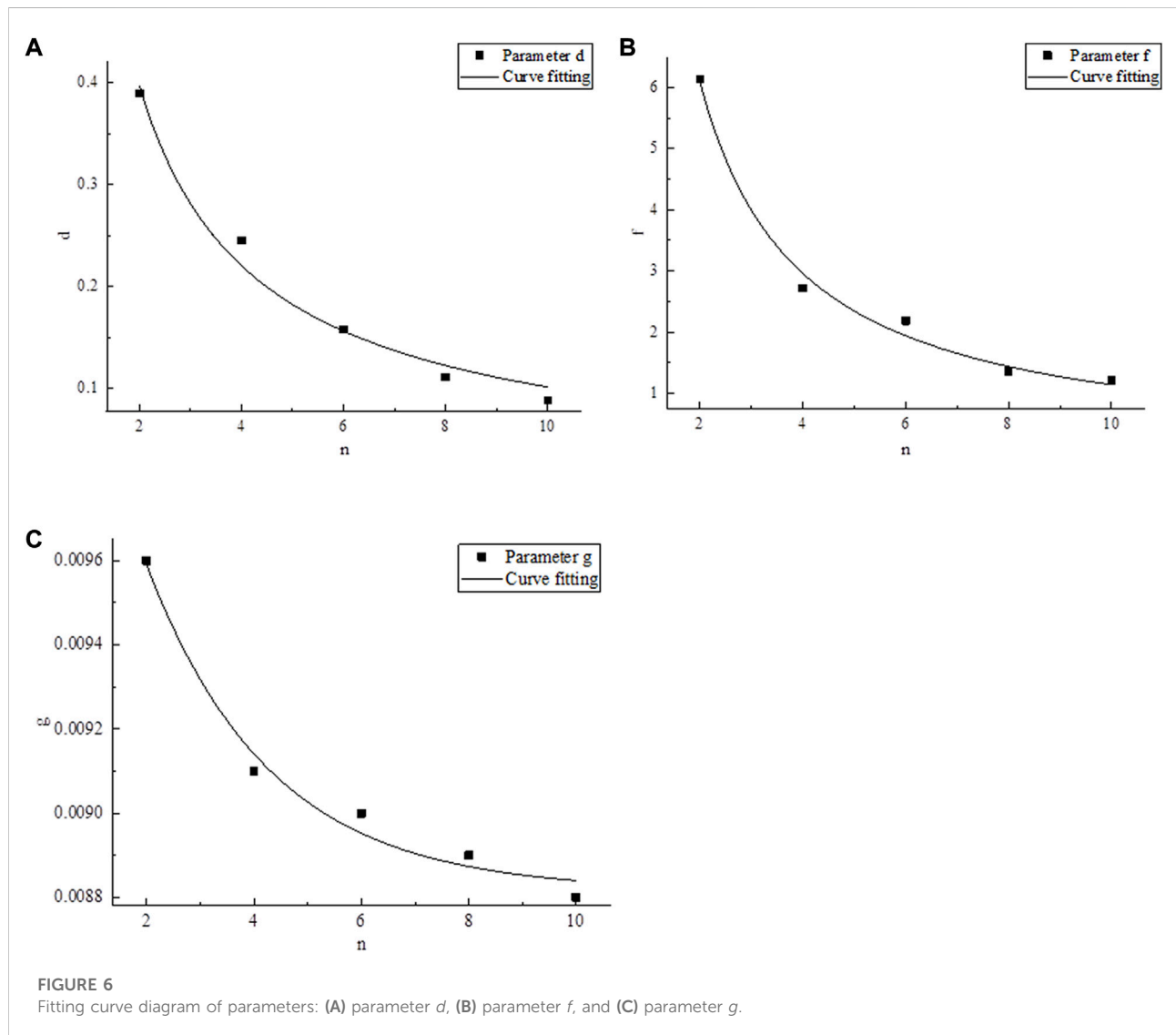


TABLE 9 Value of the characteristic size of the secant modulus.

NPJ	2	4	6	8	10
CSSM [mm]	736.564	681.909	663.791	616.937	609.122

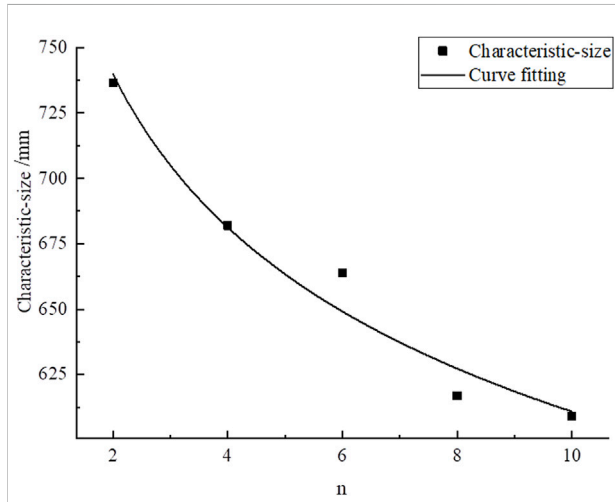


FIGURE 7 Fitting curve between CSSM and NPJs.

quantifies it and can quickly solve the E_{50} value of different rock sizes. For the engineering site, once the number of parallel joints contained in the rock is known, for any selected size of the rock, the secant modulus value of the rock under this size can be quickly solved.

3.3 Established relationship of CSBM, CBM, and NPJs

3.3.1 Formula of the characteristic size of E_{50}

The size effect of E_{50} is usually characterized by the characteristic size of the secant modulus (CSSM). Ling et al. (2013) gave a quantitative calculation method of the characteristic size. The formula for solving the CSSM is as follows:

$$|k| = |gfe^{(-gl)}|, \tag{10}$$

$$|k| \leq \gamma, \tag{11}$$

$$l \geq \frac{\ln(gf) - \ln \gamma}{g}, \tag{12}$$

where γ is the acceptable absolute value of the slope.

TABLE 10 Value of the characteristic secant modulus of the rock.

NPJ	2	4	6	8	10
CSM [GPa]	0.394	0.250	0.164	0.117	0.094

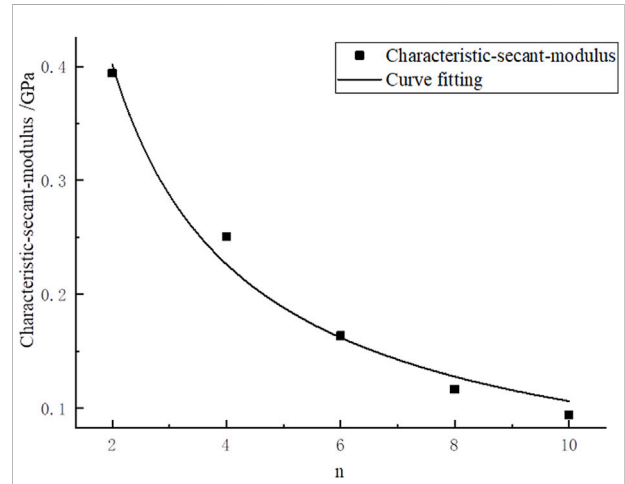


FIGURE 8 Fitting curve of the CSM and NPJs.

3.3.2 Relationship between CSSM and NPJs

The CSSM is solved in Table 9 when the NPJs were 2, 4, 6, 8, and 10. Also, the regression curve of CSSM and NPJs is drawn in Figure 7.

Figure 7 shows that there is a relationship between the CSBM and NPJs. The function of the curve is a power function. As the NPJs increase, the CSBM decreases. The expression can be obtained as

$$D(n) = 803.355n^{-0.119}, \tag{13}$$

where $D(n)$ [mm] is the characteristic size of rock E_{50} .

Eq. 13 is a special relational formula used to solve the corresponding rock CSSM when the NPJs changes, and its applicable condition is a two-dimensional plane strain. For the engineering site, the corresponding rock CSSM can be quickly obtained according to the NPJs existing in the rock. This relationship quantifies and simplifies the solution of CSSM with parallel joints, which has an important engineering application value.

3.3.3 Relationship between the CSM and NPJs

The value of CSSM was substituted into Eq. 5, and the characteristic secant modulus (CSM) with different NPJs is summarized in Table 10.

TABLE 11 Secant modulus (Liu et al., 2020).

Number of joints	Secant modulus/GPa							
	0.05 m	0.1 m	0.5 m	1 m	5 m	10 m	20 m	30 m
1	35.9	34.1	30.5	29	25.8	24.6	23.4	22.7

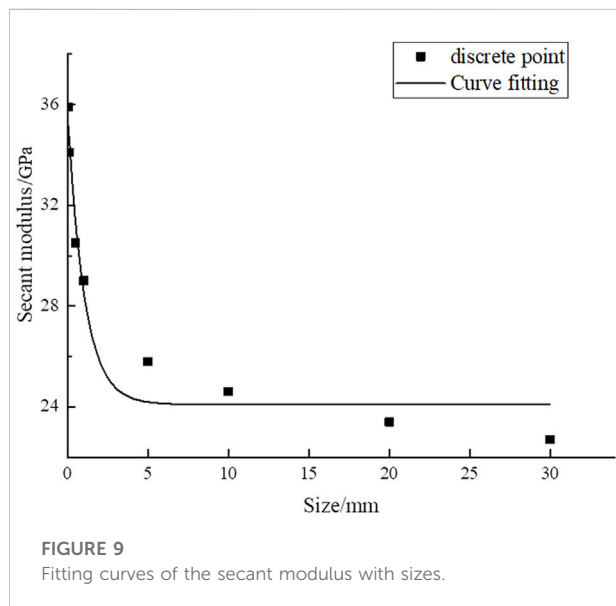


Figure 8 shows that the relationship between the CSM and NPJs is a power function. As the NPJs increase, the CSM gradually decreases. The relation is as follows:

$$E_{50w}(n) = 0.713n^{-0.827}, \quad (14)$$

where $E_{50w}(n)$ [GPa] is the CSM of the rock and n is the NPJs.

Equation 14 is a special relational formula used to solve the corresponding rock CSM when the NPJs changes, and its applicable condition is a two-dimensional plane strain. For the engineering site, the corresponding rock CSM can be quickly obtained according to the NPJs existing in the rock. This relationship quantifies and simplifies the solution of the CSM with NPJs.

3.4 Experimental comparison and verification analysis

To verify the general applicability of Eq. 5, Zhang (Zhang, 2011) experimental data (page 645, Table 1) are used. Rock E_{50} values with different sizes are listed in Table 11.

From the data listed in Table 11, a scatter diagram of E_{50} and sizes is plotted, and their fitting curves are regressed, as shown in Figure 9.

The relationship between E_{50} and sizes is obtained in Figure 9 as follows:

$$E_{50}(l) = 24.09 + 11.57e^{-0.957l}, \quad (15)$$

where $E_{50}(l)$ [GPa] is the E_{50} value of the rock when the rock size is l and l [m] is the rock size.

The function of Eq. 15 conforms to the expression proposed in Eq. 5. Therefore, the verification is consistent with the conclusions obtained from the numerical simulations in this study. According to the verification results, the mathematical model obtained by Eq. 5 can be used to solve E_{50} with different sizes.

4 Discussion

There is a size effect on E_{50} with the NPJs. This study obtains the following relationship through research:

- 1) The relation between rock E_{50} and NPJs. The relation is proposed by analyzing the variation of E_{50} with the NPJs. According to previous research studies, Zhang (2009) studied the effect of the NPJs on E_{50} based on the meso-deformation characteristics of fractured rock mass, but he did not get the specific relational formula of E_{50} . The relationship (4) obtained in this study quantifies and simplifies the solution of rock E_{50} with NPJs and can be used to solve the corresponding rock E_{50} value when the parallel joint changes. For the engineering site, when the size of the rock used for research is determined, the corresponding rock secant modulus value can be quickly obtained according to the number of parallel joints existing in the rock.
- 2) The relation between rock E_{50} and the rock size. This relationship is proposed by analyzing the variation of rock E_{50} with the rock size. According to previous research studies, scholars mostly obtained the general law of the size effect of E_{50} from the perspectives of the rock aspect ratio (Asgari et al., 2015), particle size (Hu et al., 2022a), and joint length (Ban et al., 2019). However,

the relationship between E_{50} and rock size is rarely established. Eq. 9 obtained in this study quantifies the size effect of E_{50} and can quickly solve E_{50} of different rock sizes. For the engineering site, the secant modulus of the rock of any size can be obtained by the regression curve, which saves the tedious process of the on-site *in situ* test, and the engineering application is simple and convenient.

- 3) The relation between the rock CSSM, CSM, and NPJs. The relationship is proposed by analyzing the variation of the CSSM and CSM with the NPJs. In the existing research, Davarpanah et al. (2020) studied the REV of E_{50} , but they did not get the specific relational formula of E_{50} . The relationships (13) and (14) obtained in this study quantify and simplify the solution of the rock CSSM and CSM with parallel joints and can be used to solve the corresponding rock CSSM and CSM when the parallel joint changes. For engineering rocks, considering the influence of the size effect, when the secant modulus of the rock needs to be calculated, it is only necessary to select rocks larger than the characteristic size for testing.

5 Conclusion

The NPJs have an effect on the E_{50} value, and few people have explored the relationship of this effect. The expressions are obtained through numerical simulation:

- (1) The relation between E_{50} and NPJs observes the following:

$$E_{50}(n) = an^b. \quad (16)$$

Particularly, our simulations obtained

$$E_{50}(n) = (0.714 + 12.437e^{-0.011})n^{2.344n-0.937}. \quad (17)$$

- (2) The relation between E_{50} and rock size with NPJs observes the following:

$$E_{50}(l) = d + fe^{-gl}. \quad (18)$$

Particularly, our simulations obtained

$$E_{50}(l) = 12.522l^{-1.04}e^{-0.00185le^{-0.434l}-0.0088l} + 0.714l^{-0.848}. \quad (19)$$

- (3) The CSSM is found to be related to NPJs. Their relation is as follows:

$$D(n) = 803.355n^{-0.119}. \quad (20)$$

- (4) The CSM is found to be related to NPJs. Their relation is as follows:

$$E_{50w}(n) = 0.713n^{-0.827}. \quad (21)$$

Data availability statement

The original contributions presented in the study are included in the article/Supplementary Material; further inquiries can be directed to the corresponding author.

Author contributions

JZ: data curation, investigation, funding acquisition, and writing—original draft preparation. WG: methodology and formal analysis. FUY: data curation and investigation. FEY: formal analysis and investigation. QW: formal analysis and data curation. GH: conceptualization, software, funding acquisition, and writing—original draft preparation. TW: data curation and investigation.

Funding

This work was supported by the Project: Inner Mongolia Dayan Mining Group Co., Ltd. entrusted “Research and Application of Two-way Profitable Balance Support Technology under High Stress Soft Rock Conditions in No. 3 Coal Mine (Research and Development of New Resin Anchoring Agent)” (GJNY-21-108), the Zhejiang Collaborative Innovation Center for Prevention and Control of Mountain Geological Hazards (PCMGH-2017-Y-05), and the Key Laboratory of Rock Mechanics and Geohazards of Zhejiang Province (ZGRMG-2019-07).

Conflict of interest

Authors FUY and FEY were employed by China Energy Investment.

The remaining authors declare that the research was conducted in the absence of any commercial or financial relationships that could be construed as a potential conflict of interest.

Publisher's note

All claims expressed in this article are solely those of the authors and do not necessarily represent those of their affiliated organizations, or those of the publisher, the editors, and the reviewers. Any product that may be evaluated in this article, or claim that may be made by its manufacturer, is not guaranteed or endorsed by the publisher.

References

- Ahn, J., Gabr, M., Oh, J., and Shin, H. (2015). Degraded secant modulus for permanent deformation of soils [J]. *Int. J. Pavement Eng.* 16 (6), 549–558.
- Asgari, M. R., Baghebanzadeh Dezfouli, A., and Bayat, M. (2015). Experimental study on stabilization of a low plasticity clayey soil with cement/lime. *Arab. J. Geosci.* 8 (3), 1439–1452. doi:10.1007/s12517-013-1173-1
- Ban, H., Yao, Y., Chen, S., and Fang, D. (2019). A new constitutive model of micro-particle reinforced metal matrix composites with damage effects. *Int. J. Mech. Sci.* 152, 524–534. doi:10.1016/j.ijmecsci.2019.01.024
- Briaud, J. L. (2001). *Introduction to soil moduli*. Richmond, B.C., Canada: BiTech Publishers Ltd. Geotechnical News.
- Davaranpanah, S. M., Somodi, G., Kovács, L., and Vasarhelyi, B. (2020). Experimental Determination of the mechanical properties and deformation Constants of Mórággy Granitic rock formation (Hungary). *Geotech. Geol. Eng. (Dordr)*. 38 (3), 3215–3229. doi:10.1007/s10706-020-01218-4
- Erisa, M., Jérôme, S., Evelyne, P., and Mohend, C. (2021). Fatigue deterioration mechanisms of high-strength grout in compression. *Constr. Build. Mater.* 270, 121387. doi:10.1016/j.conbuildmat.2020.121387
- Hang-Zhou, L. I., and Liao, H. J. (2007). Experimental study on Nonlinear strength deformation characteristic of Expansive mudstone [J]. *Chin. J. Undergr. Space Eng.* 3 (1), 19–22.
- Hu, G., Ma, G., Liang, W., Song, L., and Fu, W. (2022). Influence of the number of parallel-joints on size Effect of Elastic modulus and characteristic Elastic modulus [J]. *Front. Earth Sci.* 10, 1–11.
- Hu, G., Ma, G., Liu, J., and Qi, K. (2022). Size Effect of the number of parallel joints on uniaxial compressive strength and characteristic strength[J]. *Minerals* 12 (1), 1–24.
- Kang, Y., Chen, J., Cheng, N., and Luo, Y. (2018). Evolution characteristics of secant modulus and its Post peak damage in three Axial compression for sandstone [J]. *J. Inn. Mong. Univ. Technol. Sci. Ed.* 37 (1), 35–42.
- Li, B., Lan, J., Si, G., Lin, G., and Hu, L. (2020). NMR-based damage characterisation of backfill material in host rock under dynamic loading. *Int. J. Min. Sci. Technol.* 30 (03), 329–335. doi:10.1016/j.ijmst.2020.03.015
- Ling, Z. Z., Zhang, Y. B., Tang, B., Li, L. C., and Tang, C. A. (2013). Size effect of rock masses and associated representative element properties. *Chin. J. Rock Mech. Eng.* 32 (6), 1157–1166.
- Liu, J., Su, H., Jing, H., Hu, C., and Yin, Q. (2020). Experimental study on the fracture Evolution Process of rock-like specimens containing a Closed Rough Joint based on 3D-Printing Technology. *Adv. Civ. Eng.* 2020 (1), 1–16. doi:10.1155/2020/8889606
- Loyola, A. C., Pereira, J. M., and Neto, M. (2021). General Statistics-based methodology for the Determination of the geometrical and mechanical representative Elementary volumes of fractured media[J]. *Rock Mech. Rock Eng.* 54, 1841–1861.
- Mahdevari, S., Moarefvand, P., and Mohammadzamani, D. (2020). Considering the Effect of Block-to-matrix strength ratio on Geomechanical parameters of Bimrocks. *Geotech. Geol. Eng. (Dordr)*. 38 (5), 4501–4520. doi:10.1007/s10706-020-01304-7
- Majdi, A., and Beiki, M. (2019). Applying evolutionary optimization algorithms for improving fuzzy C-mean clustering performance to predict the deformation modulus of rock mass. *Int. J. Rock Mech. Min. Sci. (1997)*. 113, 172–182. doi:10.1016/j.ijrmms.2018.10.030
- Nouri, S., Nechnech, A., Lamri, B., and Lurdes Lopes, M. (2016). Triaxial test of drained sand reinforced with plastic layers. *Arab. J. Geosci.* 9 (1), 53. doi:10.1007/s12517-015-2017-y
- Peng, C., Guo, Q., Yan, Z., Wang, M., and Pan, J. (2020). Investigating the failure mechanism of jointed rock slopes based on Discrete Element method. *Adv. Civ. Eng.* 2020 (9), 1–19. doi:10.1155/2020/8820158
- Su, H., Jing, H., Yin, Q., Yu, L., Wang, Y., and Wu, X. (2017). Strength and deformation behaviors of veined marble specimens after vacuum heat treatment under conventional triaxial compression. *Acta Mech. Sin.* 33 (5), 886–898. doi:10.1007/s10409-017-0653-z
- Sun, Z., Wu, Y., Sun, J., Chen, J., Fu, Y., and Shan, S. (2022). Aspect ratio effect of dynamic deformation modulus of coal under three-dimensional dynamic and static loading [J]. *J. Min. Rock Form. Control Eng.* 4 (04), 67–77.
- Wang, X., Kang, H., and Gao, F. (2021). Numerical study on the formation of pressure arch in bolted gravel plate. *Comput. Geotechnics* 130 (2021), 103933. doi:10.1016/j.compgeo.2020.103933
- Zhang, L., and Zhu, J. (2020). Analysis of mechanical strength and failure Morphology of prefabricated Closed cracked rock mass under uniaxial compression [J]. *Geotechnical Geol. Eng.* 38 (B6), 1–11.
- Zhang, T., Liu, N., Pang, M., Zhang, X., Wang, X., and Zhang, X. (2021). Influence of temperature and stress on compaction deformation characteristics of broken coal and rock mass[J]. *Coal Mine Saf.* 52 (06), 58–64+71.
- Zhang, T. (2013). *Research on the anisotropy of rock mass mechanical parameter REV in underground cavern storage [D]*. Wuhan: China University of Geosciences.
- Zhang, Y., Xia, Z., Jiang, Y., Chen, M., Liu, J., and Yin, Q. (2020). Effect of Hole density and confining pressure on mechanical behavior of porous specimens: An Insight from Discrete Element modeling. *Comput. Model. Eng. Sci.* 125 (1), 259–280. doi:10.32604/cmes.2020.011076
- Zhang, Z. (2011). Research on dimensional Effect of deformation modulus of underground Cavern rock mass [J]. *J. Eng. Geol.* 19 (05), 642–647.
- Zhang, Z. (2009). *Micro-characteristics of failure of non-penetrating fractured rock mass and determination method of its macro-mechanical parameters [D]*. Xi'an: Xi'an University of Technology.
- Zhao, L., Li, Z., Liu, G., Pang, X., and Tian, C. (2017). Study on parameter values of modified Mohr-Coulomb model for granite residual soil[J]. *Railw. Constr.* 17 (03), 89–92.
- Zhu, X. (2021). *Experimental study on constitutive model parameters of hardened soil in typical sand and pebble strata in Beijing area[D]*. Beijing: Beijing Jiaotong University.